Raman-active phonons in $Bi_2Sr_2Ca_{1-x}Y_xCu_2O_{8+d}$ ($x=0-1$): Effects of hole filling and internal pressure induced by Y doping for Ca, and implications for phonon assignments

Masato Kakihana and Minoru Osada
Research Laboratory of Engineering Materials, Tokyo Institute of Technology, 4259 Nagatsuta, Midori-ku, Yokohama 226, Japan

Mikael Käll
Department of Solid State Physics, Risø National Laboratory, DK-4000 Roskilde, Denmark

Lars Börjesson
Department of Applied Physics, Chalmers University of Technology, S412-92 Göteborg, Sweden

Hiromasa Mazaki and Hiroshi Yasuoka
Department of Mathematics and Physics, The National Defense Academy, 1-10-20 Hashirimizu Yokosuka 239, Japan

Masatomo Yashima and Masahiro Yoshimura
Research Laboratory of Engineering Materials, Tokyo Institute of Technology, 4259 Nagatsuta, Midori-ku, Yokohama 226, Japan
(Received 28 August 1995; revised manuscript received 15 January 1996)

The phonon Raman spectra of $Bi_2Sr_2Ca_{1-x}Y_xCu_2O_{8+d}$ ($x=0-1$) have been investigated in a number of well-defined single-crystal and polycrystalline samples. From the polarization and Y-doping dependence, and from a comparison with previous reports on Bi-based cuprates, we identify the ($6A_{1g}+1B_{1g}$) symmetry modes that are Raman allowed within the ideal body-centered-tetragonal unit cell. A large number of extra ''*disorder-induced*'' phonon bands are observed in the *ab*-plane polarized spectra. In contrast to most previous reports, we argue that the *c*-axis polarized phonon band around 629 cm^{-1} is due to the $O(2)_{Sr}$ A_{1g} vibration, while the exclusively *ab*-plane polarized band around 463 cm^{-1} is induced by the $O(3)_{Bi}$ A_{1g} vibration. With increasing Y doping we find that the vibrational modes involving atoms in the CuO_2 planes rapidly increase in intensity as a result of the reduced metallic screening in the hole-depleted Y-doped samples. We also find that Y substitution gives rise to a substantial hardening of the $O(1)_{Cu}$ A_{1g} and B_{1g} phonons by ~ 40 cm^{-1}, whereas the $O(2)_{Sr}$ A_{1g} phonon is found to soften by ~ 20 cm^{-1}, when x increases from 0 to 1. The phonon frequency changes can be explained by the ''*internal pressure*'' induced by the decrease in the average Ca/Y ion size and an additional ''*charge-transfer*'' induced by the change in the Cu and Bi valences with Y doping.

I. INTRODUCTION

Aliovalent cation substitutions in cuprates have provided valuable insight into the mechanisms that give rise to high-T_c superconductivity. Most important is the possibility of substantially altering the effective copper valence and the carrier concentration, which have been shown to be intimately linked with T_c. The prototypic example is the Sr-substituted $La_{2-x}Sr_xCuO_4$ system.[1] A striking feature here is the existence of a plateau with nearly constant critical temperature, in which the carrier concentration is optimized for the occurrence of superconductivity. A similar phase diagram has also been found when Y is substituted for Ca in the $Bi_2Sr_2Ca_{1-x}Y_xCu_2O_{8+d}$ (Bi2212) compound.[2–4] A relatively sharp metal-insulator transition takes place between $x=0.45$ and 0.55, giving rise to the antiferromagnetic order similarly found in the La_2CuO_4 (Ref. 5) and $YBa_2Cu_3O_6$ (Ref. 6) insulators. The normal-state resistivity systematically increases with increasing Y concentration, implying a decreased number of charge carriers consistent with reported Hall-effect measurements.[7,8] The depression of T_c and the decreasing carrier concentration have been interpreted as a result of hole filling due to the additional electrons contributed by the trivalent Y^{3+} ion relative to the divalent Ca^{2+} ion. This interpretation is mainly based on detailed oxygen stoichiometric analyses[2,9,10] which show that the amount of oxygen uptake is insufficient to balance the extra charge introduced by Y^{3+}.

One way to obtain further understanding of the doping process in $Bi_2Sr_2Ca_{1-x}Y_xCu_2O_{8+d}$ would be to investigate the change in the optical-phonon spectrum with Y content. Phonon Raman scattering has provided valuable information on the effects of, e.g., oxygen deficiency,[11–13] Pr substitution for Y,[14] and substitutions on the two Cu sites[15–17] in the $YBa_2Cu_3O_{7-d}$ superconductor. Although a variety of spectroscopic studies on $Bi_2Sr_2Ca_{1-x}Y_xCu_2O_{8+d}$ have been reported in the literature[7,18–24] there are a limited number of Raman-scattering studies.[25–28] Sugai and Sato[25,26] reported additional phonons as well as broad two-magnon peaks induced by Y doping, while Boekholt and co-workers[27,28] reported an intensity resonance for certain phonons at an incident laser energy of 2.6 ± 0.1 eV in single crystals with $x=0-0.85$.

In order to use Raman scattering as a tool for investigations of the high-T_c compounds, it is important to be able to correctly assign the experimentally observed phonon modes to vibrational eigenmodes of the lattice. This has turned out to be quite difficult in Bi2212, and a number of discrepancies

exist among previous reports.[29–44] Difficulties arise both from the orthorhombic distortion, the incommensurate superstructural modulation[45,46] as well as from complicated local atomic distortions away from the ideal symmetry sites.[47,48] These effects induce many more phonon modes than is expected from the symmetry of the idealized body-centered-tetragonal unit cell. One example of the ambiguities involved in phonon assignments comes from the single-crystal Raman works on $Bi_2Sr_2Ca_{1-x}Y_xCu_2O_{8+d}$ cited above:[25–28] one group[27,28,30] assigned the intense 463- and 629-cm^{-1} phonons to the in-phase O_{Cu} A_g mode and the O_{Sr} A_g mode, respectively, while the other group[25,26,32,40] assigned the low-frequency phonon to the O_{Sr} A_g mode and the high-frequency phonon to the O_{Bi} A_g mode. In these works no c-axis-polarized spectra were reported, even though this scattering configuration is expected to be the most informative for vibrations along the c axis. Except for a few examples,[30,33,44] this is also the case for unsubstituted Bi2212.

The aim of the present study is twofold: on the one hand, we try to partly resolve some previous ambiguities regarding the phonon assignments in Bi2212, and on the other hand we try to interpret the change in the phonon Raman spectrum with Y doping. We present results for single crystals as well as for high-quality polycrystalline samples with varying degree of Y doping x, particularly focusing on the two most prominent oxygen vibrational modes at 463 and 629 cm^{-1}. In order to clarify the assignments of the 463 and 629-cm^{-1} phonons, we have studied Raman spectra of our single crystals under the $x(zz)\bar{x}$ scattering configuration as well as the $z(xx)\bar{z}$ or $z(yy)\bar{z}$ scattering configuration. On the basis of the phonon assignments proposed here, we interpret the observed changes in phonon frequencies and intensities with increasing Y content in terms of a combination of an ''*internal-pressure*'' effect, induced by the change in the average Ca/Y radius, and a ''*charge-transfer*'' effect, induced by the aliovalent substitution of Y^{3+} for Ca^{2+}.

II. EXPERIMENTS

The polycrystalline $Bi_2Sr_2Ca_{1-x}Y_xCu_2O_{8+d}$ samples with Y content in the range $0 \leqslant x \leqslant 1$ were synthesized by a polymerized complex technique described in detail elsewhere.[3,49] This method is known to give very pure and homogeneous cuprate superconductors.[3,49]

The samples were characterized by x-ray powder diffraction (XRPD) using a standard powder x-ray diffractometer (Model MXP^{3VA}, Cu $K\alpha$, 40 kV–40 mA, MAC Science, Japan). The scan rate was 0.5°/min. The lattice parameters of some selected samples ($0 \leqslant x \leqslant 1$) were determined by least-squares fits of the positions of the reflection peaks with Si powder (99.999%) for the angular calibration.

The superconducting transitions of the polycrystalline samples were investigated by measuring the complex magnetic susceptibility, $\chi = \chi' - i\chi''$, as a function of temperature. A Hartshorn bridge was used to measure χ' and χ'' simultaneously in an ac magnetic field $h(t) = h^0 \sin(2\pi ft)$ with $f = 132$ Hz and $h^0 = 100$ mOe. The onset of the superconducting transition can be precisely determined by this technique, as it corresponds to the off-balance temperature of the carefully zero-balanced bridge (for details see Ref. 50).

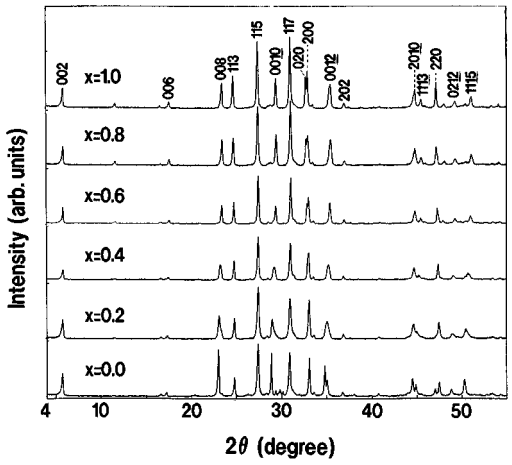

FIG. 1. X-ray powder-diffraction patterns, using Cu $K\alpha$ radiation, $Bi_2Sr_2Ca_{1-x}Y_xCu_2O_{8+d}$ polycrystalline samples prepared by the polymerized complex technique. Numbers shown are indices corresponding to (h,k,l) reflections from the orthorhombic unit cell (and the pseudotetragonal unit cell for $x < 0.4$).

Single crystals of $Bi_2Sr_2Ca_{1-x}Y_xCu_2O_{8+d}$ with x values close to 0, 0.4, 0.6, and 0.8 were grown from the stoichiometric melt composition, as described in a separate publication.[51] Typical crystals dimensions were $\sim 2 \times 2 \times 0.1$ mm^3.

We used two different experimental setups for the Raman-scattering measurements of $Bi_2Sr_2Ca_{1-x}Y_xCu_2O_{8+d}$. In the first setup, consisting of a Jobin Yvon/Atago Bussan T64000 triple spectrometer equipped with microscope optics, we performed room-temperature Raman measurements using either the microprobe (mostly for small single crystals) or a standard macro configuration (mostly for polycrystalline samples). Low-temperature measurements were performed with small pieces of polycrystalline samples mounted on the cold finger of a liquid-helium cryostat, using a Raman microprobe coupled to a Spex 1877 spectrometer. A backscattering configuration was used in both the experimental setups. All Raman spectra were excited with the 5145-Å line of an Ar laser, and the scattered light was detected with liquid-nitrogen-cooled CCD cameras. The power of the incident laser beam was maintained below roughly 100 W/cm^2 in order to minimize possible thermal damage. The spectral resolution was 3–4 cm^{-1}. Throughout this paper the scattering configuration is defined by notations such as $x(zz)\bar{x}$, which means that the incident light polarized along the z axis propagates along the x axis, and the scattered light polarized along the z axis propagates along the opposite x axis (i.e., $\bar{x}$). The coordinates (x,y,z) are chosen to coincide with the crystallographic axes (a,b,c).

III. SAMPLE CHARACTERIZATION

Figure 1 shows typical x-ray powder-diffraction (XRPD) patterns of the polycrystalline $Bi_2Sr_2Ca_{1-x}Y_xCu_2O_{8+d}$ material. These patterns show that the samples are pure and of single phase within the experimental accuracy ($< 1-2$ %). In particular we find no traces of $Bi_2Sr_2CuO_y$, Ca_2CuO_y, CuO, $Y_2Cu_2O_5$ or CaO, which are the most frequently

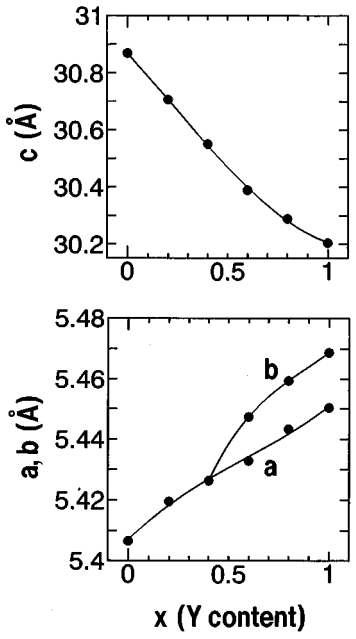

FIG. 2. Variation of the $a(b)$ and c lattice parameters of $Bi_2Sr_2Ca_{1-x}Y_xCu_2O_{8+d}$ as a function of Y content, x. The parameters up to $x=0.4$ can be indexed on the basis of a pseudotetragonal unit cell, and for $x>0.4$ they can be indexed on the basis of an orthorhombic unit cell, as is evident by the splitting of the (2,0,0) and (0,2,0) reflections ($2\theta=33°$) in the XRPD patterns (see Fig. 1).

formed as by-products in the synthesis of the Bi2212 phase. This result is confirmed by the Raman-scattering measurements, which are sensitive to traces of semiconducting or insulating impurities.[49]

For high Y content, $x>0.4$, the XRPD patterns were indexed on the basis of an orthorhombic unit cell; the orthorhombic distortion being evident through the splitting of the (2,0,0) and (0,2,0) reflections ($2\theta=33°$). For low Y content, $x\leqslant 0.4$, the XRPD patterns exhibited broadened (2,0,0) and (0,2,0) reflections, indicating a small orthorhombic distortion with b slightly larger than a, but no clear splitting. In those cases the diffraction patterns were indexed by a pseudotetragonal cell with $a=b$.

Figure 2 shows the change in the lattice parameters of the $Bi_2Sr_2Ca_{1-x}Y_xCu_2O_{8+d}$ samples as a function of x. As the Y content increases from $x=0$ to 1, the c parameter decreases monotonically by $\sim 2.26\%$, while the a (and a, b for $x>0.4$) parameter increases by $\sim 1\%$. The values shown in Fig. 2 are in good agreement with previous reports.[4,7]

As an example of a typical complex magnetic susceptibility measurement, we show in Fig. 3 the temperature dependence of χ' and χ'' for the polycrystalline $Bi_2Sr_2Ca_{0.8}Y_{0.2}Cu_2O_{8.21}$ sample. T_c (onset) at $T=91.6$ K is followed by a sharp transition corresponding to the weak-link coupling between the bulk superconducting grains. The diamagnetic signal is almost completely saturated at about 10 K below T_c (onset); the transition width (10–90 %) being about 3.5 K. A single loss peak with a maximum at about 87 K is observed in the χ'' part of the magnetic susceptibility, indicating a monophase superconductor within the resolution of the susceptibility measurement. Figure 4 shows T_c (onset)

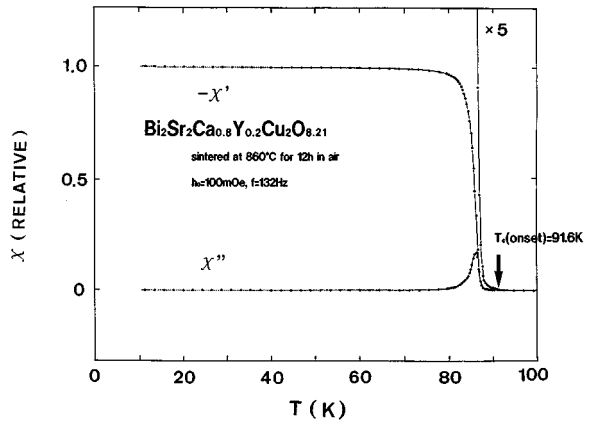

FIG. 3. Real (χ') and imaginary (χ'') components of χ vs temperature for a polycrystalline sample of $Bi_2Sr_2Ca_{0.8}Y_{0.2}Cu_2O_{8.21}$. The amplitude of the applied field is 100 mOe. The onset temperature is 91.6 K (indicated by an arrow). The χ' is almost completely saturated at a temperature lower than T_c (onset) by approximately 10 K; the transition width (10–90 %) of the full diamagnetism being about 3.5 K. A single loss peak with a maximum at about 87 K is observed in the χ'' component.

for the $x=0-0.4$ samples. It is evident that the critical temperature reaches a maximum of about 92 K between $x=0.1$ and 0.3. For sample with $x>0.5$ no superconductivity was found down to 4 K. The relation between T_c and x found here is similar to what has been reported earlier by several other groups.[2–4,7–9]

IV. RESULTS

A body-centered-tetragonal structure ($I4/mmm$) with the primitive cell shown in Fig. 5 has been most frequently used in the interpretation of the Raman spectra of Bi2212 as a first approximation for the real structure. The group-theoretical analysis based on this idealized structure[52] predicts 14 Raman-active modes ($6A_{1g}+1B_{1g}+7E_g$), where the A_{1g} modes are symmetric c-axis vibrations of Bi, Sr, Cu,

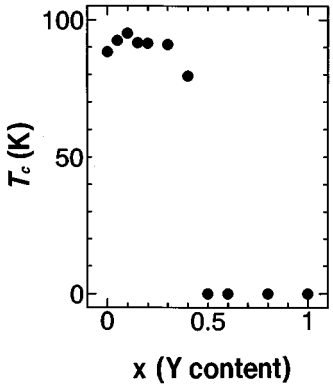

FIG. 4. The variation of the superconducting transition onset temperature (T_c) of $Bi_2Sr_2Ca_{1-x}Y_xCu_2O_{8+d}$ as a function of Y content, x. The T_c (onset)'s were determined in a way similar to that described in Fig. 3.

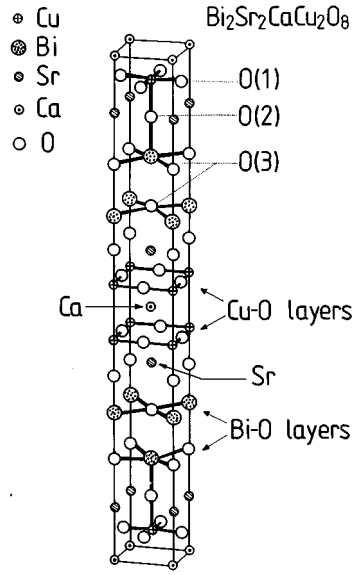

FIG. 5. Idealized crystal structure of the body-centered-tetragonal ($I4/mmm$) $Bi_2Sr_2CaCu_2O_8$. O(1), O(2), and O(3) represent oxygens in the Cu, Sr, and Bi layers, respectively.

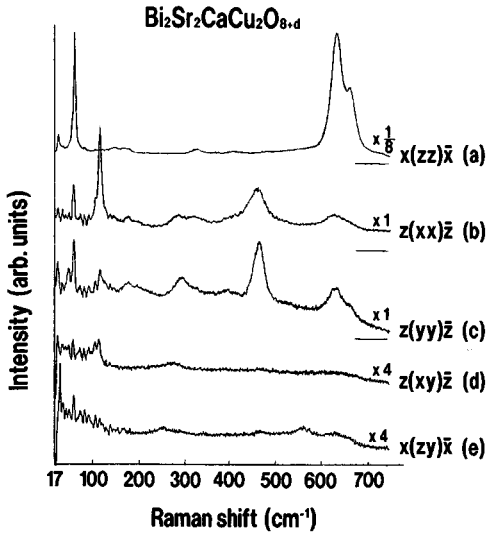

FIG. 6. Polarized micro-Raman spectra of a $Bi_2Sr_2CaCu_2O_{8+d}$ single crystal from five main scattering configurations. The short lines denote the zero-intensity level for the spectrum immediately above. The scattering factors are also shown. Note the different scattering factors. Many additional lines observed below 150 cm^{-1}, most notably in (b)–(e), are originated from the pure rotational lines of N_2 and O_2 in ambient air. As the position of these rotational lines are precisely known, they can be discriminated from the true Raman lines from Bi2212.

$O(1)_{Cu}$, $O(2)_{Sr}$, and $O(3)_{Bi}$, the B_{1g} mode is an out-of-phase vibration of the $O(1)_{Cu}$ atoms along the c axis, and the E_g modes are vibrations within the ab plane. However, the fact that the number of observed modes largely exceeds that expected from the $I4/mmm$ tetragonal structure requires that the phonon Raman spectrum of Bi2212 should be interpreted within a crystal structure of lower symmetry. Possible origins of this symmetry reduction involve (i) the orthorhombic distortion, (ii) the incommensurate superstructural modulation along the b axis, and (iii) large atomic displacements and substantial disorder, all of which can yield additional Raman modes. We refer to these modes as ''*disorder-induced*'' modes, and do not specify their origin. We note that several groups have applied factor-group analyses based on the orthorhombic space groups $Bbmb$ and $Amaa$ [which yields $12A_g+7B_{1g}$ (Refs. 25 and 40) and $12A_g+8B_{1g}$ (Refs. 30, 32, and 33) c-axis modes, respectively] in order to interpret the complicated ab-plane-polarized spectra of Bi2212. Since it is not clear which orthorhombic space group best describes the complicated atomic distortions in Bi2212, we will only use the ideal tetragonal notation.

A. Phonon Raman spectra of undoped $Bi_2Sr_2CaCu_2O_{8+d}$

Typical Raman spectra at room temperature of a $Bi_2Sr_2CaCu_2O_{8+d}$ single crystal under the five main scattering configurations are shown in Fig. 6 in the 17–745 cm^{-1} range. The symmetric A_{1g} modes can be detected under the $x(zz)\bar{x}$, $z(xx)\bar{z}$, and $z(yy)\bar{z}$ scattering configurations. Under crossed polarization $z(xy)\bar{z}$ the A_{1g} modes should disappear, instead of which B_{1g} modes can be investigated. The $x(zy)\bar{x}$ spectrum of Fig. 6 exhibits a few broad and weak E_g symmetry phonons around $\sim$250, $\sim$470, and $\sim$570 cm^{-1}. The frequencies of the observed A_{1g} and B_{1g} symmetry phonons are tabulated in Table I, together with our proposed assignment. A part of our data is also compared with results of previously published single-crystal investigations.[25,30,32,33,40]

The most prominent result is that the two phonons at 60 and 629/657 cm^{-1} are strongly c-axis polarized, as is evident in the $x(zz)\bar{x}$ spectrum [Fig. 6(a)]. Their intensities are approximately 25 times higher than those observed under both the $z(xx)\bar{z}$ and the $z(yy)\bar{z}$ scattering configurations. We assign the 629/657 cm^{-1} phonon pair to A_{1g}-symmetry vibrations of the bridging oxygen $O(2)_{Sr}$ along the c-axis (see below). From simple mass considerations, the intense phonon at 60 cm^{-1} can be assigned to the A_{1g}-symmetry vibration of the heavy Bi atom. The extremely large intensities of the Bi and $O(2)_{Sr}$ A_{1g} modes indicate that the polarizability of the Bi-$O(2)_{Sr}$ bond is unusually high.

The mode at 463 cm^{-1}, which is completely absent in the $x(zz)\bar{x}$ spectrum [Fig. 6(a)], is usually assigned to the bridging $O(2)_{Sr}$ vibration along the c axis. As discussed below, the 463-cm^{-1} phonon should instead be assigned to the $O(3)_{Bi}$ A_{1g} mode of the BiO layers.

From the B_{1g}-symmetry selection rules the peak at 287 cm^{-1}, which occurs only in the $z(xy)\bar{z}$ spectrum [Fig. 6(d)], can be assigned to the $O(1)_{Cu}$ B_{1g} phonon[25,26,28,30,32] characterized by out-of-phase motion of the oxygen atoms in the CuO_2 plane. This mode exhibits a pronounced asymmetry induced by a Fano interference between the phonon and an electronic scattering background.

The assignments of Sr and Cu A_{1g} modes are made by comparison with other high-T_c superconductors.[53,54] The peak at 117 cm^{-1} is probably related to A_{1g} vibrations of Sr. In the real structure this mode involves a significant contri-

TABLE I. Phonon frequencies and assignments of the phonon Raman modes in $Bi_2Sr_2CaCu_2O_{8+d}$.

Present work			Liu *et al.* (Ref. 40)		Cardona *et al.* (Ref. 32)		Sugai and Sato (Ref. 25)		Boekholt *et al.* (Ref. 30)			Denisov *et al.* (Ref. 33)		
Assign.[j]	*ab* plane[a]	*c* axis[b]	Assign.[l]	*ab* plane	Assign.[k]	*ab* plane	Assign.[l]	*ab* plane	Assign.[k]	*ab* plane	*c* axis	Assign.[k]	*ab* plane	*c* axis
c	24	27	e	28				29						
d	48		f	47			Bi	53						
Bi A_{1g}	**59**	**60**	Bi[i]	62			Bi[i]	63	Bi	63		Bi	65	65
(Bi/Sr)[h]	105		Cu[i]	109										
Sr A_{1g}	**117**		Bi	119	Bi	122	Sr	121	Sr	120		Sr	122	120
(Bi/Sr)[h]	129		Cu	129	Bi[i]	133	Sr[i]	132						
Cu A_{1g}	**145**	**146**	Sr[i]	180	Sr	156	Cu	142	Cu	165		Cu	175	
Cu[h]	175	173	Sr	180	Cu	184	Cu[i]	187	Cu[i]	190		Cu	200	
(Bi/Sr)[h]	195				(Sr,Cu)[i]	219								
O_{Cu} B_{1g}	**287**		O_{Cu} B_{1g}	285	O_{Cu} B_{1g}	282	O_{Cu} B_{1g}	289	O_{Cu} B_{1g}	275		O_{Cu} B_{1g}	280	
($O_{Bi}O_{Sr}$)[h]	294		O_{Bi}[i]	295	$O_{Bi\ bend}$	296	O_{Sr}[i]	293	$O_{Bi\ bend}$	290		O_{Cu}	300	
($O_{Bi}O_{Sr}$)[h]	323	325				313	O_{Cu}[i]	327	g	313	313	O_{Cu}		320
($O_{Bi}O_{Sr}$)[h]	353		O_{Cu}[i]	355				359						
($O_{Bi}O_{Sr}$)[h]	395		O_{Sr}[i]	400	O_{Cu}	391	O_{Cu}	394				O_{Bi}		400
O_{Cu} A_{1g}	**409**	**409**												
O_{Bi} A_{1g}	**463**		O_{Sr}	465	O_{Sr}	469	O_{Sr}	469	O_{Cu}	463		O_{Bi}	460	
O_{Sr} A_{1g}	**627**	**629**	O_{Bi}	630	O_{Bi}	631	O_{Bi}	632	O_{Sr}	625		O_{Sr}	634	634
O_{Sr}[h]	656	657	g	660	g	659	O_{Bi}	663	O_{Sr}[i]	650	650	O_{Bi}[i]	655	655

[a]Scattering configurations; $z(xx)\overline{z}$ or $z(yy)\overline{z}$ (A_{1g},A_g), and $z(xy)\overline{z}$ (B_{1g}).

[b]Scattering configuration; $x(zz)\overline{x}$ (A_{1g},A_g).

[c]Acoustic mode or the mode induced by the superstructural modulation.

[d]Bi mode induced by the orthorhombic distortion or the mode induced by the superstructural modulation.

[e]The mode induced by the superstructural modulation.

[f]Second-order mode of 28 cm^{-1} mode.

[g]O_{extra} or folded mode in O_{Bi}.

[h]Tetragonal forbidden modes (''*disorder-induced*'' modes).

[i]Tetragonal forbidden modes (or modes induced by the orthorhombic distortion).

[j]Phonon assignments based on an ideal tetragonal structure $I4/mmm$.

[k]Phonon assignments based on the orthorhombic space group $Amaa$.

[l]Phonon assignments based on the orthorhombic space group $Bbmb$.

bution from Bi because of its large anisotropic behavior seen in the $z(xx)\bar{z}$ and $z(yy)\bar{z}$ spectra of Figs. 6(b) and 6(c). The weak peak at 145 cm^{-1} involves A_{1g} motions mostly of Cu. One of bases of this assignment has come from the fact that the peak at 145 cm^{-1} gains intensities considerably when the material becomes an insulator by substituting Y for Ca in a way similar to oxygen-depleted $YBa_2Cu_3O_{7-d}$ (Y123).[11–13] This will be discussed later.

Most phonons observed below 400 cm^{-1} in the $z(xx)\bar{z}$ and $z(yy)\bar{z}$ spectra of Fig. 6 can be associated with ''*disorder-induced*'' scattering. For instance, the weak peaks at 105, 129, and 195 cm^{-1} most likely involve displacements of Bi and Sr, since these atoms should be more sensitive to the deviation from the tetragonal symmetry than the Cu atoms. Likewise, the broad features between ~200 and ~400 cm^{-1} should be dominated by $O(3)_{Bi}$ and $O(2)_{Sr}$ vibrations. The two low-frequency peaks at 24 and 48 cm^{-1} have been interpreted as folded acoustic modes or amplitude modes, induced by the superstructural modulation.[40,41] Although both of these modes are highly (yy) polarized, i.e., in the direction of the modulation, we note that the 24-cm^{-1} mode also has a significant (zz) component [see Fig. 6(a)].[55]

B. Phonon Raman spectra of $Bi_2Sr_2Ca_{1-x}Y_xCu_2O_{8+d}$

In Fig. 7 we show Raman spectra of polycrystalline $Bi_2Sr_2Ca_{1-x}Y_xCu_2O_{8+d}$ samples for different degrees of Y doping at room temperature and $T=20$ K. Figures 8–10 exhibit room-temperature Raman spectra of several single crystals samples in various scattering configurations. The following important observations should be pointed out:

(i) When the Y content increases, the B_{1g} $O(1)_{Cu}$ phonon rapidly increases in intensity [Figs. 7(a) and 9] and in frequency, as shown in Fig. 11(a). The B_{1g} $O(1)_{Cu}$ mode also becomes more and more symmetric with increasing x, as can be seen in the $z(xy)\bar{z}$ spectra of Fig. 9. A weak feature around ~409 cm^{-1}, which is most evident in the 20 K spectra of Fig. 7(b), also increases in frequency by about 40 cm^{-1} [see Fig. 11(b)] and becomes much more intense when the Y content is increased. The similarity to the $O(1)_{Cu}$ B_{1g} mode in this respect suggests that the ~409-cm^{-1} feature is in fact the $O(1)_{Cu}$ A_{1g} mode, i.e., the in-phase vibration of the $O(1)_{Cu}$ atom along the c axis. Similarly, modes connected with Cu motions at 145 and 177 cm^{-1} progressively gain intensities with increasing Y content (Fig. 8).

(ii) The $O(3)_{Bi}$ c-axis phonon band contains one intense mode at 468 cm^{-1} (463 cm^{-1} at 290 K) as well as a prominent shoulder at 458 cm^{-1} in the 20 K spectrum, where the phonon thermal broadening is small [Fig. 7(b)]. Their relative intensities, I_{458}/I_{468}, systematically increase with increasing Y doping.

(iii) The 629/657 cm^{-1} phonon pair softens strongly with increasing Y content [Figs. 7 and 10]. The frequency change for the polycrystalline samples is plotted as a function of Y content in Fig. 11(c).

V. DISCUSSION

A. What is the origin of the 463- and 629-cm^{-1} phonons?

We first address the controversial assignments of the two prominent high-frequency oxygen A_{1g} symmetry modes at about 463 and 629 cm^{-1}. The single-crystal spectra of Fig. 6 have revealed that these two bands exhibit completely different polarization dependencies; the 463-cm^{-1} band is only seen when the incident and scattered polarization vectors lie within the *ab* plane, while the 629-cm^{-1} band is strongly c-axis polarized. This indicates that the phonons in question modulate different metal-oxygen bonds, i.e., the degree of mode mixing is small. We first note that the assignment of the 463-cm^{-1} phonon to a CuO_2-plane vibration[30] cannot be correct, since this phonon (as well as the 629-cm^{-1} mode) also appears in Raman spectra of Bi2201[40,56–58] where the CuO_2 planes have inversion symmetry and therefore do not contribute any Raman-allowed modes. We assign the 629-

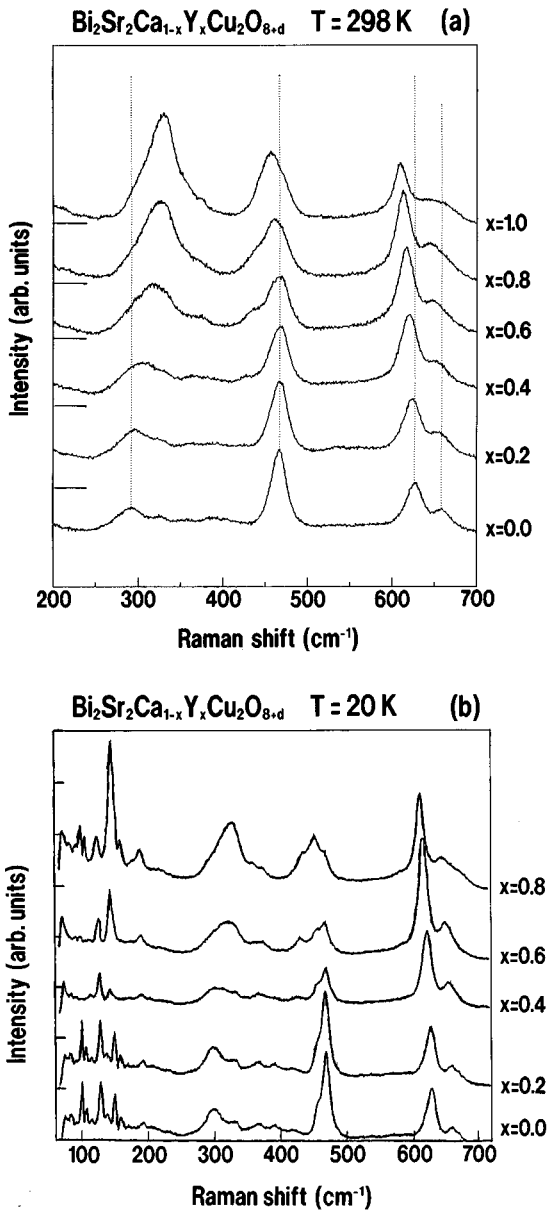

FIG. 7. Raman spectra of $Bi_2Sr_2Ca_{1-x}Y_xCu_2O_{8+d}$ polycrystalline samples for different Y contents at room temperature (a) and $T=20$ K (b). The spectra can be presumed to be made up by the superposition of the $z(xx)\bar{z}$ and $z(yy)\bar{z}$ spectra with more contribution from the former. The short lines denote the zero-intensity level for the spectrum immediately above.

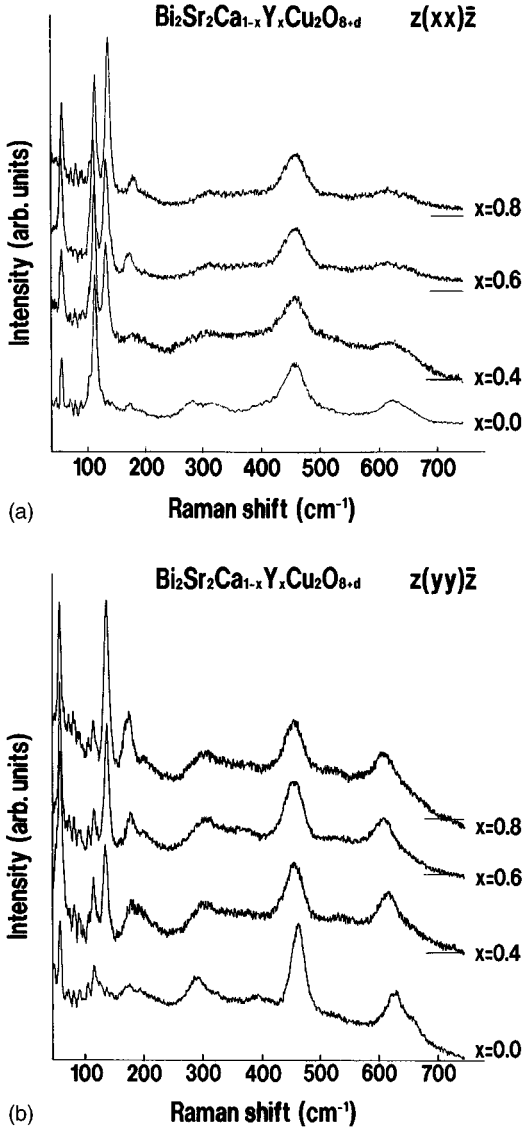

FIG. 8. Polarized micro-Raman spectra at the A_{1g} symmetry [under the $z(xx)\bar{z}$ (a) and $z(yy)\bar{z}$ (b) scattering configurations] taken on the *ab* plane of $Bi_2Sr_2Ca_{1-x}Y_xCu_2O_{8+d}$ single crystals with $x=0$, 0.4, 0.6, and 0.8. The short lines denote the zero-intensity level for the spectrum immediately above.

cm^{-1} phonon to symmetric A_{1g} vibrations of $O(2)_{Sr}$ along the *c* axis, while the 463-cm^{-1} band is assigned to $O(3)_{Bi}$ A_{1g} *c*-axis vibrations (in agreement with Denisov *et al.*[33]). There are several reasons why this is a more likely alternative than the reversed assignment made in several previous reports.

First, a predominantly (zz)-polarized apex oxygen vibration is characteristic for most high-T_c superconductors,[53,54] which indicate that the exclusively $x(zz)\bar{x}$-polarized 629-cm^{-1} phonon in Bi2212 is due to the $O(2)_{Sr}$ vibration. The fact[59] that the (zz)-polarized spectrum of $BiSr_2CaCu_2O_y$ (Bi1212), with no Raman-active modes in the BiO layers, shows a very strong mode at 627 cm^{-1} also supports our interpretation of the 629-cm^{-1} phonon in Bi2212. The recent Raman work on Bi2212 samples with the Sr site homovalently substituted by Ca (Ref. 60) has shown that the

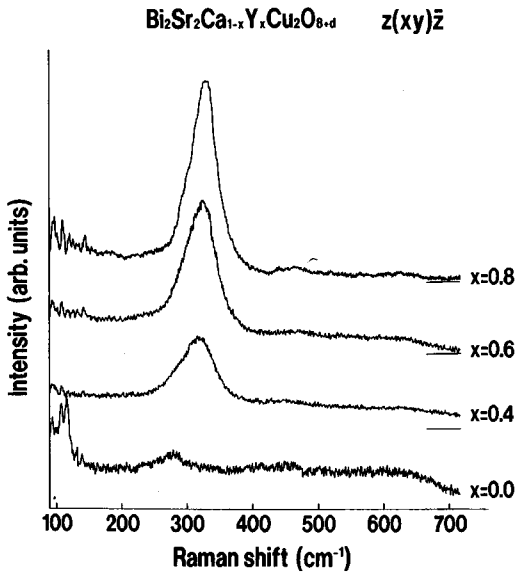

FIG. 9. Polarized micro-Raman spectra of the B_{1g} symmetry [under the $z(xy)\bar{z}$ scattering configuration] taken on the *ab* plane of $Bi_2Sr_2Ca_{1-x}Y_xCu_2O_{8+d}$ single crystals with $x=0$, 0.4, 0.6, and 0.8. The short lines denote the zero-intensity level for the spectrum immediately above.

629-cm^{-1} mode shifts to higher energy when Sr is replaced by Ca, whereas the mode at about 463 cm^{-1} remains unchanged upon the substitution, as can be expected from the assignments suggested here. We also note that the 463-cm^{-1} band has been found to soften at a significantly faster rate than the 629-cm^{-1} band when ^{18}O is exchanged for

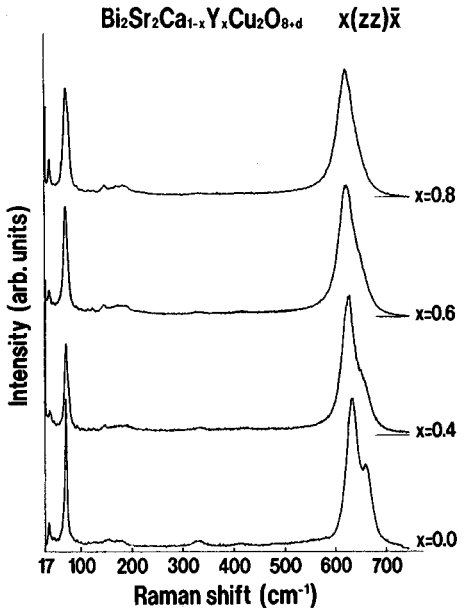

FIG. 10. Polarized micro-Raman spectra of the A_{1g} symmetry [under the $x(zz)\bar{x}$ scattering configuration] taken on the *bc* plane of $Bi_2Sr_2Ca_{1-x}Y_xCu_2O_{8+d}$ single crystals with $x=0$, 0.4, 0.6, and 0.8. The short lines denote the zero-intensity level for the spectrum immediately above.

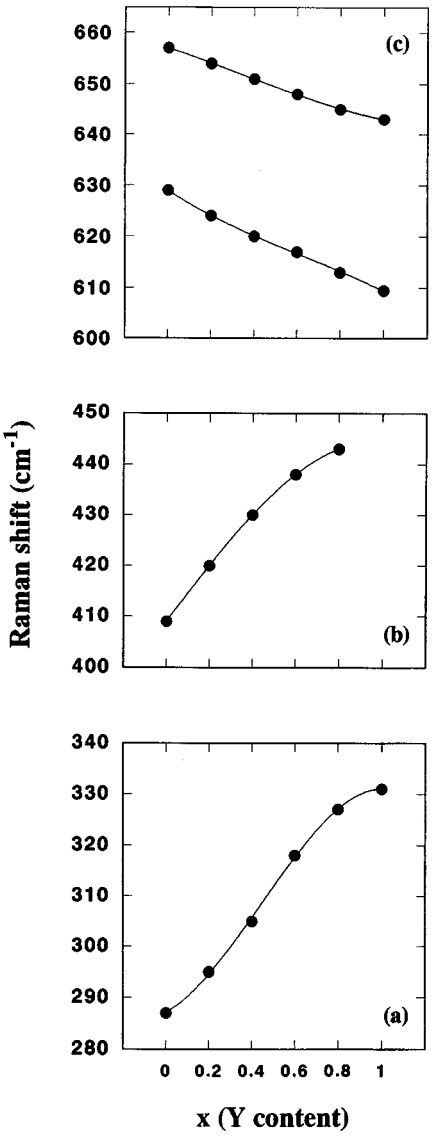

FIG. 11. Variation of frequencies for the B_{1g} 287 cm^{-1} $O(1)_{Cu}$ (a), the A_{1g} 409 cm^{-1} $O(1)_{Cu}$ (b) and A_{1g} 629/657 cm^{-1} $O(2)_{Sr}$ (c) modes in $Bi_2Sr_2Ca_{1-x}Y_xCu_2O_{8+d}$ polycrystalline samples [observed in Fig. 7(a)]. Solid lines are only a guide for the eye.

^{16}O in $Bi_2Sr_2Ca_{0.8}Y_{0.2}Cu_2O_{8+d}$.[37] In view of the fact that loss and uptake of oxygen take place in the BiO layers,[47,48] this indicates that the 463-cm^{-1} phonon is connected with the more labile oxygen atoms in the BiO layer, in agreement with our assignments.

On the other hand, the origin of the splitting of the two high-frequency phonons, i.e., the appearance of the sidebands at ~458 cm^{-1} [see Fig. 7(b)] and 657 cm^{-1} (see, e.g., Fig. 10), remains unsettled. One possibility is that the splitting reflects a distribution of $O(2)_{Sr}$-Bi-$O(3)_{Bi}$ force constants induced by the incommensurate superstructural modulation. The fact that the 657-cm^{-1} phonon disappears in the Raman spectra of modulation-free $Bi_{2-x}Pb_xSr_2CaCu_2O_{8+d}$ (Refs. 29, 36, and 42) and $Bi_{2-x}Pb_xSr_2Ca_{1-y}Y_yCu_2O_{8+d}$,[61] where the Bi-$O(2)_{Sr}$ bonds should be vertically aligned in a more ordered way, may support this idea. Another possibility is that the sidebands are induced by extra oxygen atoms in the BiO layers. The substitution of Y for Ca indeed increases the amount of oxygens,[9,10] which can considerably alter the local structure of the BiO layer.[62] This could then explain the drastic increase in the I_{458}/I_{468} ratio with increasing Y doping.

B. Effects of hole filling and internal pressure on some of phonons in $Bi_2Sr_2Ca_{1-x}Y_xCu_2O_{8+d}$

Two interesting aspects of the phonon Raman spectra of $Bi_2Sr_2Ca_{1-x}Y_xCu_2O_{8+d}$ are discussed below in conjunction with the metal-insulator transition induced by the Y doping. We pay attention to the behaviors of the bridging-oxygen $O(2)_{Sr}$ mode and of modes involving atoms in the CuO_2 planes.

As shown in Fig. 11(c), the frequencies of the 629/657 cm^{-1} $O(2)_{Sr}$ phonon pair decrease almost already linearly by about ~20 cm^{-1} when the Y content increases from $x=0$ to $x=1$. The situation appears to be similar to what has been reported for the $R123$ system,[63,64] where the corresponding O_{Ba} A_g mode softens when the size of the R ion decreases [from 514 cm^{-1} for $R=$Nd ($r_{Nd^{3+}}=1.109$ Å) to 501 cm^{-1} for $R=$Tm ($r_{Tm^{3+}}=0.994$ Å)]. This softening can be explained by the expansion of the Cu_{plane}-O_{Ba} bond length (from ~2.249 Å in Nd123 to ~2.290 Å in Tm123) in response to the contraction around the R ion (the $Cu_{chain}O_{Ba}$ bond length is ≈1.860 Å for all R).[65] Since the Ca site in $Bi_2Sr_2CaCu_2O_{8+d}$ has a local structure crystallographically similar to the R site in $RBa_2Cu_3O_{7-d}$, the same structural arguments can, *at least partly*, explain the behavior of the $O(2)_{Sr}$ phonons in Y-doped Bi2212; i.e., the replacement of the large Ca ion by the small Y ion should result in an elongation of the Cu-$O(2)_{Sr}$ bond length, which in turn explains the decrease in the $O(2)_{Sr}$ phonon frequencies. Unfortunately, there seems to be no reliable reports on interatomic bond lengths in Y-doped Bi2212, that can substantiate this hypothesis. It is also possible that ''*charge-transfer*'' effects, associated with the change in Ca^{2+}/Y^{3+} average valence with x, contribute to the $O(2)_{Sr}$ phonon softening, in a fashion similar to what has been observed for the O_{Ba} mode in oxygen-depleted Y123 (Refs. 11–13) and in Co-doped Y123.[15–17] The origin of the softening in both the Y123 systems is thought to be due to changes in the distribution of charge between CuO chains and the CuO_2 planes.[15,66] This type of charge redistribution occurs in the Y-doped Bi2212. In fact coulometric titration experiments[9,10] have shown that the valences of both Bi and Cu decrease for increasing x (from $Bi^{+3.2}/Cu^{+2.18}$ for $x=0$ to $Bi^{+3.0}/Cu^{2.05}$ for $x=1$), which should then weaken the Cu-$O(2)_{Sr}$-Bi bond. The rate of $O_{Ba/Sr}$ phonon softening is indeed faster in Bi2212 (≈−3.2% per 0.1 Å decrease in Ca/Y average ion size) than in $R123$ (≈−2.3% per 0.1 Å decrease in R ion size), which may indicate that both ''*internal-pressure*'' and ''*charge-transfer*'' effects are important in the former system.

The CuO_2-plane phonons are of particular interest, as they concern atoms directly involved in the superconductivity. We have identified four CuO_2-plane phonons (at 145, 177, 409, and 287 cm^{-1}). All these modes are weak in superconducting metallic samples ($x\leq 0.4$), while their intensities increase dramatically with decreasing metallicity

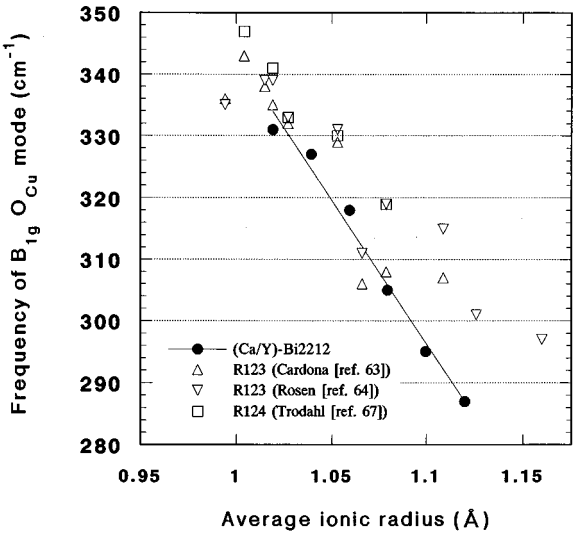

FIG. 12. Variation with the (average) ionic radius of the frequency of the B_{1g} $O(1)_{Cu}$ mode of $Bi_2Sr_2Ca_{1-x}Y_xCu_2O_{8+d}$ (solid circles). For a comparison, the corresponding B_{1g} O_{Cu} frequency for $RBa_2Cu_3O_{7-d}$ [open triangles (Refs. 63 and 64)] and $RBa_2Cu_4O_8$ [open squares (Ref. 67)] are also plotted in the same figure. The solid line is only a guide for the eye.

($x \geqslant 0.6$) as can be seen in, e.g., Figs. 7–9. The B_{1g} 287 cm^{-1} phonon becomes more and more symmetric with increasing Y doping. These effects are most probably direct manifestations of the decrease in the number of charge carriers induced by Y doping. The smaller number of holes in the Y-substituted samples both leads to a reduced metallic screening within and between adjacent CuO_2 layers, leading to larger CuO_2 bond polarizabilities and phonon intensities, and to a weaker electronic Raman background resulting in a less prominent Fano asymmetry. Similar effects have also been observed for the corresponding vibrations related to the CuO_2 planes in $YBa_2Cu_3O_{7-d}$ when oxygen is removed from the structure.[11–13]

Figure 11(a) shows that the $O(1)_{Cu}$ B_{1g} phonon hardens dramatically by $\sim$40 cm^{-1} when the Y content increases from $x=0$ to $x=1$. Figure 12 shows the variation of the phonon frequency with the average Ca^{2+}/Y^{3+} ionic radius for the different compositions x. We also compare with what has been reported for the corresponding O_{Cu} B_{1g} mode in $RBa_2Cu_3O_{7-d}$ ($R$123; R=rare-earth elements)[63,64] and $RBa_2Cu_4O_8$ ($R$124).[67] The similarity between the Bi2212 and $R$123/124 systems is striking. For the latter systems the change in the O_{Cu} B_{1g} phonon frequency can be explained by the change in size of the R^{3+} ions, since the electronic properties are more or less independent of the type of R ion (with the exception of R=Pr).[14,68] Smaller R ions result in a contraction of the O_{Cu}-Cu and O_{Cu}-R bonds, larger force constants and a higher phonon frequency. Moreover, since the frequency of the B_{1g} O_{Cu} mode increases by only $\sim$5 cm^{-1} on going from the superconducting $YBa_2Cu_3O_7$ to the nonsuperconducting $YBa_2Cu_3O_6$, the change in Cu valence does not largely affect the energy of the B_{1g} O_{Cu} phonon in the $R$123 system. From this view point, the hardening of the B_{1g} $O(1)_{Cu}$ mode in $Bi_2Sr_2CaCu_2O_{8+d}$ with Y substitution can be primarily explained in terms of the change in the average Ca/Y radius analogous to $R$123 (or $R$124). The similarity between the Bi2212 system and the $R$123/124 systems in this respect thus suggests that additional factors, such as the increase in average Ca^{2+}/Y^{3+} valence and the decrease in the hole concentration with Y doping, only have a small influence on the B_{1g} $O(1)_{Cu}$ phonon frequency. The structural arguments discussed above also explain the hardening of the $O(1)_{Cu}$ A_{1g} mode at 409 cm^{-1} [see Fig. 11(b)] by $\sim$40 cm^{-1} from $x=0$ to $x=1$.

VI. CONCLUSION

The phonon Raman spectra of $Bi_2Sr_2Ca_{1-x}Y_xCu_2O_{8+d}$ single crystals and polycrystalline samples have been investigated over the full compositional range: $x=0-1$. Single-crystal room-temperature measurements were performed in the five main polarization geometries, including the ''difficult'' c-axis-polarized geometry. Additional measurements of polycrystalline samples have been performed at room temperature and at $T=20$ K. For $x<0.5$ the samples were found to be superconducting, with a maximum T_c of $\approx$92 K for $0.1<x<0.3$. From the dependence on polarization directions and Y doping, and from a comparison with other Bi-based cuprates, we identify the $(6A_{1g}+1B_{1g})$ symmetry modes that are Raman allowed within the ideal body-centered-tetragonal unit cell (space group $I4/mmm$). A number of additional ''*disorder-induced*'' phonon bands occur in the *ab*-plane-polarized spectra. For increasing degree of Y doping we find that the Cu A_{1g} mode at 145 cm^{-1}, the $O(1)_{Cu}$ B_{1g} mode at 287 cm^{-1}, and the $O(1)_{Cu}$ A_{1g} mode at 409 cm^{-1} increase dramatically in intensity. We attribute this effect to the reduced metallic screening in the CuO_2 planes, that can be expected in the hole-depleted Y-doped samples. The decreasing carrier concentration also manifests itself in the disappearance of the Fano asymmetry of the $O(1)_{Cu}$ B_{1g} mode. The $O(1)_{Cu}$ and $O(2)_{Sr}$ phonons exhibit substantial frequency changes with Y doping. While the two $O(1)_{Cu}$ modes harden by $\sim$40 cm^{-1}, the $O(2)_{Sr}$ A_{1g} mode at 629 cm^{-1} softens $\sim$20 cm^{-1} between $x=0$ and $x=1$. These frequency changes, which are similar to what has been reported for the corresponding modes in the $RBa_2Cu_3O_{7-d}$ superconductor for decreasing rare-earth ion size, are mainly of a structural origin. For increasing x, the decrease in the average Ca/Y radius is expected to cause an ''*internal pressure*'' on the $O(1)_{Cu}$ atoms and an elongation of the Cu-$O(2)_{Sr}$ bond length which results in the observed phonon frequency changes. In the case of the $O(2)_{Sr}$ A_{1g} mode it is also possible that additional but non-negligible ''*charge-transfer*'' effects contribute to the phonon softening.

ACKNOWLEDGMENTS

The authors would like to thank Dr. M. Kawai (The Institute of Physical and Chemical Research) and Dr. R. Sekine (Tokyo Institute of Technology) for fruitful discussions. M.

Kakihana would like to thank the President of the Tokyo Institute of Technology, who financed this work by a special college research fund. M. Osada gratefully acknowledges the financial support of the Japan Society for the Promotion of Science. This work is financially supported by the Swedish Natural Science Research Council and by a Grant-in-Aid for Scientific Research (No. 4482) from the Ministry of Education, Science and Culture of Japan.

[1] J. B. Torrance, Y. Tokura, A. I. Nazzal, A. Bezinge, T. C. Huang, and S. S. Parkin, Phys. Rev. Lett. **61**, 1127 (1988).
[2] A. Manthiram and J. B. Goodenough, Appl. Phys. Lett. **53**, 420 (1988).
[3] H. Mazaki, M. Kakihana, and H. Yasuoka, Jpn. J. Appl. Phys. **30**, 38 (1991).
[4] T. Tamegai, K. Koga, K. Suzuki, M. Ichihara, F. Sakai, and Y. Iye, Jpn. J. Appl. Phys. **28**, L112 (1989).
[5] N. Nishida, N. Miyatake, D. Shimada, S. Okuma, M. Ishikawa, T. Takabatake, Y. Nakazawa, Y. Kuno, R. Keitel, J. H. Brewe, T. M. Riseman, D. L. Williams, Y. Watanabe, T. Yamazaki, K. Nishiyama, K. Nagamine, E. J. Ansaldo, and E. Torikai, Jpn. J. Appl. Phys. **26**, L1856 (1987).
[6] J. M. Tranquada, D. E. Cox, W. Kunnmam, H. Moudden, G. Shirane, M. Suenaga, P. Zolliker, D. Vaknin, S. K. Sinha, M. S. Alvarez, A. J. Jacobsen, D. C. Johnston, Phys Rev. Lett. **60**, 156 (1988).
[7] A. Maeda, M. Hase, T. Tsukada, K. Noda, S. Takebayashi, and K. Uchinokura, Phys. Rev. B **41**, 6418 (1990).
[8] W. A. Groen, D. M. de Leeuw, and L. F. Feiner, Physica C **165**, 55 (1990).
[9] T. Kawano, F. Munakata, H. Yamauchi, and S. Tanaka, J. Mater. Res. **7**, 299 (1992).
[10] M. Karppinen, A. Fukuoka, J. Wang, S. Takano, M. Wakata, T. Ikemachi, and H. Yamauchi, Physica C **208**, 130 (1993).
[11] M. Hangyo, S. Nakashima, K. Mizoguchi, A. Fujii, A. Mitsuishi, and T. Yotsuya, Solid State Commun. **65**, 835 (1988).
[12] R. Liu, C. Thomsen, W. Kress, M. Cardona, B. Gegenheimer, F. W. de Wette, J. Prade, A. D. Kulkarni, and U. Schröder, Phys. Rev. B **37**, 7971 (1988).
[13] C. Thomsen, R. Liu, M. Bauer, A. Wittlin, L. Genzel, M. Cardona, E. Schönherr, W. Bauhofer, and W. König, Solid State Commun. **65**, 55 (1988).
[14] H. G. Radously, K. F. McCarty, J. L. Peng, and R. N. Shelton, Phys. Rev. B **39**, 12 383 (1989).
[15] M. Kakihana, L. Börjesson, S. Eriksson, P. Svedlindh, and P. Norling, Phys. Rev. B **40**, 6787 (1989).
[16] M. Kakihana, S. Eriksson, L. Börjesson, C. Ström, L. G. Johansson, and M. Käll, Phys. Rev. B **47**, 5359 (1993).
[17] L. Börjesson, L. Van Hong, M. Käll, M. Kakihana, and P. Berastegui, J. Alloys Compounds **195**, 363 (1993).
[18] A. Q. Pham, N. Merrien, A. Maignan, F. Studer, C. Michel, and B. Raveau, Physica C **210**, 350 (1993).
[19] C. S. Gopinath, S. Subramanian, P. S. Prabahu, M. S. Ramachandra, and G. V. S. Rao, Physica C **218**, 117 (1993).
[20] R. Itti, F. Munakata, K. Ikeda, H. Yamauchi, N. Koshizuka, and S. Tanaka, Phys. Rev. B **43**, 6249 (1991).
[21] T. Takahashi, H. Matsuyama, H. Katayama-Yoshida, K. Seki, K. Kamiya, and H. Inokuchi, Physica C **170**, 416 (1990).
[22] D. Mandrus, L. Forro, D. Koller, and L. Mihaly, Nature (London) **351**, 460 (1991).
[23] A. J. Pal, P. Mandal, A. Poddar, and B. Ghosh, Physica C **181**, 186 (1991).
[24] L. Forro, G. L. Carr, G. P. W. Williams, D. Mandrus, and L. Mihaly, Phys. Rev. Lett. **65**, 1941 (1990).
[25] S. Sugai and M. Sato, Jpn. J. Appl. Phys. **28**, L1361 (1989).
[26] S. Sugai and M. Sato, Phys. Rev. B **40**, 9292 (1989).
[27] M. Boekholt, G. Güntherodt, L. I. Leonyuk, and V. V. Moshchalkov, Physica C **185-189**, 1035 (1991).
[28] M. Boekholt, G. Güntherodt, and V. V. Moshchalkov, Physica C **192**, 191 (1992).
[29] L. Ben-Dor, M. Y. Szerer, G. Blumberg, A. Givan, L. Börjesson, and L. V. Hong, Physica C **200**, 418 (1992).
[30] M. Boekholt, A. Erle, P. C. Splittgerber-Hünnekes, and G. Güntherodt, Solid State Commun. **74**, 1107 (1990).
[31] G. Burns, G. V. Chandrashekhar, F. H. Dacol, and P. Strobel, Phys. Rev. B **39**, 775 (1989).
[32] M. Cardona, C. Thomsen, R. Liu, H. G. von Schnering, M. Hartweg, Y. F. Yan, and Z. X. Zhao, Solid State Commun. **66**, 1225 (1988).
[33] V. N. Denisov, B. N. Mavrin, V. B. Podobedov, I. V. Alexandrov, A. B. Bykov, A. F. Goncharov, O. K. Mel'nikov, and N. I. Romanova, Solid State Commun. **70**, 885 (1989).
[34] L. A. Farrow, L. H. Greene, J.-M. Tarascon, P. A. Morris, W. A. Bonner, and G. W. Hull, Phys. Rev. B **38**, 752 (1988).
[35] E. Fauliques, P. Dupouy, and S. Lefrant, J. Phys. (France) I **1**, 901 (1991).
[36] P. V. Huong, R. Cavagnat, A. L. Verma, K. Kitahama, T. Kawai, M. Lahaye, and E. Marquestaut, J. Alloys Compounds **195**, 133 (1993).
[37] B. K. Kim, M. Kakihana, M. Yashima, M. Yoshimura, S. J. Park, and H. Hamaguchi, Phys. Rev. B **49**, 15 388 (1994).
[38] D. Kirillov, I. Bozovic, T. H. Geballe, A. Kapitulnik, and D. B. Mitzi, Phys. Rev. B **38**, 11 955 (1988).
[39] P. Knoll, B. Stadlober, M. Pressl, and N. Brnicevic, Physica C **162-164**, 1097 (1989).
[40] R. Liu, M. V. Klein, P. D. Han, and D. A. Payne, Phys. Rev. B **45**, 7392 (1992).
[41] S. Martinez, A. Zwick, M. A. Renucci, H. Noel, and M. Potel, Physica C **200**, 307 (1992).
[42] J. Sapriel, J. Schneck, J. F. Scott, J. C. Toledano, L. Pierre, J. Chavignon, C. Daguet, J. P. Chaminade, and H. Boyer, Phys. Rev. B **43**, 6259 (1991).
[43] M. Stavola, D. M. Krol, L. F. Schneemeyer, S. A. Sunshine, R. M. Fleming, J. V. Waszczak, and S. G. Kosinski, Phys. Rev. B **38**, 5110 (1988).
[44] A. Yamanaka, H. Takato, F. Minami, K. Inoue, and S. Takekawa, Physica C **185-189**, 1027 (1991).
[45] C. C. Torardi, J. B. Parise, M. A. Subramanian, J. Gopalakrishnan, and A. W. Sleight, Physica C **157**, 115 (1989).
[46] H. W. Zandbergen, W. A. Groen, F. C. Mijlhoff, G. van Tendeloo, and S. Amelinckx, Physica C **156**, 325 (1990).
[47] P. Bordet, J. J. Capponi, C. Chaillout, J. Chenavas, A. W. Hewat, E. A. Hewat, J. L. Hodeau, M. Marezio, J. L. Tholence, and D. Tranqui, Physica C **156**, 189 (1988).
[48] A. Yamamoto, M. Onoda, E. Takayama-Muromachi, F. Izumi, T.

Ishigaki, and H. Asano, Phys. Rev. B **42**, 4228 (1990).
[49] M. Kakihana, J. Sol-Gel Sci. Technol. **6**, 7 (1996).
[50] T. Ishida and H. Mazaki, Phys. Rev. B **20**, 131 (1979).
[51] M. Osada, M. Kakihana, H. Mazaki, H. Yasuoka, M. Yashima, and M. Yoshimura (unpublished).
[52] J. Prade, A. D. Kulkarni, F. W. de Wette, U. Schröder, and W. Kress, Phys. Rev. B **39**, 2771 (1989).
[53] C. Thomsen and M. Cardona, in *Physical Properties of High Temperature Superconductors I*, edited by Donald M. Ginsberg (World Scientific, Singapore, 1989), and references therein.
[54] C. Thomsen, in *Light Scattering in Solids VI*, edited by M. Cardona and G. Güntherodt (Springer-Verlag, Berlin, 1991), and references therein.
[55] The 24-cm^{-1} line has also been observed in another 4880-Å excitation, which excludes the possibility that the 24-cm^{-1} line is due to a plasma line from the laser.
[56] K. C. Hewitt, A. Martin, Y. H. Shi, and M. J. G. Lee, Physica C **216**, 463 (1993).
[57] M. Zhiqiang, Z. Hongguang, T. Mingliang, T. Sun, X. Yang, W. Yu, Z. Jian, X. Chunyi, and Z. Yuheng, Phys. Rev. B **48**, 16 135 (1993).
[58] C. V. Narasimha Rao, H. J. Trodahl, and J. L. Tallon, Physica C **225**, 45 (1994).
[59] P. V. Huong, C. Lacour, and M. M'Hamdi, J. Alloys Compounds **195**, 691 (1993).
[60] R. Sekine, Y. Murakoshi, M. Kawai, M. Kakihana, M. Yashima, M. Kudo, and S. Teratani (unpublished).
[61] M. Osada, M. Kakihana, S. Eriksson, C. Ström, M. Käll, L. Börjesson, M. Yashima, and M. Yoshimura (unpublished).
[62] H. W. Zandbergen, W. A. Groen, F. C. Mijlhoff, G. van Tendeloo, and S. Amelinckx, Physica C **156**, 325 (1988).
[63] M. Cardona, R. Liu, C. Thomsen, M. Bauer, L. Genzel, W. König, A. Wittlin, U. Amador, M. Barahona, F. Fernandez, C. Otero, and R. Saez, Solid State Commun. **65**, 71 (1988).
[64] H. J. Rosen, R. M. Macfarlane, E. M. Engler, V. Y. Lee, and R. D. Jacowitz, Phys. Rev. B **38**, 2460 (1988).
[65] M. Guillaume, P. Allenspach, W. Henggeler, J. Mesot, B. Roessli, U. Staub, P. Fischer, and V. Trounov, J. Phys. **6**, 7963 (1994).
[66] J. D. Jorgensen, B. W. Veal, A. P. Paulikas, L. J. Nowicki, G. W. Crabtree, H. Claus, and W. K. Kwok, Phys. Rev. B **41**, 1863 (1990).
[67] H. J. Trodahl, R. G. Buckley, and C. K. Subramaniam, Phys. Rev. B **47**, 11 354 (1993).
[68] N. Watanabe, S. Adachi, S. Tajima, H. Yamauchi, and N. Koshizuka, Phys. Rev. B **48**, 4180 (1993).